moderate pressures and discussions on the ratio of viscosities of D_2O over those of H_2O will be reported in the succeeding report.

Glossary

A	constant in eq 2
C	capillary constant, cm^4
L	length of the capillary, cm
m	kinetic energy correction factor (inlet-length correction factor)
ΔP	pressure drop, Pa
Q	volumetric flow rate, cm^3/s
t	temperature difference, °C
v	specific volume, cm^3/g
z_c	compressibility factor at the critical point
α	thermal expansion coefficient, $°C^{-1}$
ν	kinematic viscosity, cm^2/s
ρ	density, g/cm^3
η	viscosity, 10^{-7}Pa s, μP

Literature Cited

(1) Agayev, N. A., Yusibova, A. D., *Dokl. Akad. Nauk SSSR*, **180**, 334 (1968).
(2) Agayev, N. A., Kerimov, A. M., Abas-Zade, A., *At. Energ.*, **30**, 534 (1971).
(3) Bonilla, C. F., Wang, S. J., Weiner, H., *Trans. ASME*, **78**, 1285 (1956).
(4) Hardy, R. C., Cottington, R. T., *J. Res. Natl. Bur. Stand.*, **42**, 573 (1969).
(5) Nagashima, A., Tanishita, I., *Bull. JSME*, **12**, 1467 (1969).
(6) Rivkin, S. L., Levin, A. Ya., Izrailevskii, L. B., Haristonov, K. G., *Teploenergetika*, **19**, 86 (1972).
(7) Rivkin, S. L., Levin, A. Ya., Izrailevskii, L. B., Haristonov, K. G., Report of IAPS Working-Group Meeting, London, 1973.
(8) Rivkin, S. L., *At. Energ.*, **7**, 457 (1959); Rivkin, S. L., Ahundov, T. C., *Teploenergetika*, **9**, 62 (1962).
(9) Schmidt, E., Ed., "Properties of Water and Steam", Springer, New York, N.Y., 1969.
(10) Su, G. J., *Ind. Eng. Chem.*, **38**, 803 (1946).
(11) Timrot, D. L., Shuiskaya, K. F., *At. Energ.*, **7**, 459 (1959).
(12) Timrot, D. L., Serednitskaya, M. A., Bespalov, M. S., *Teploenergetika*, **21**, 83 (1973).
(13) Tsederberg, N. V., Alexsandrov, A. A., Hasanshin, T. S., *Teploenergetika*, **19**, 65 (1972); **20**, 13 (1973).

Received for review August 1, 1977. Accepted October 8, 1977.

Properties of Potassium Sulfate Aqueous Solution and Crystals

Tsutomu Ishii* and S. Fujita
Department of Chemical Engineering, Tokyo Institute of Technology, Tokyo, Japan

The properties of aqueous K_2SO_4 solutions and crystals had been measured. The saturation concentrations and the first and second supersaturation concentrations of K_2SO_4 solution were measured. Densities and viscosities of concentrated K_2SO_4 solutions were measured and diffusivity data for K_2SO_4 in solution were correlated by Wilke's diffusion factor. Specific surface area and shape factors for K_2SO_4 crystals were measured.

The properties of aqueous concentrated K_2SO_4 solution and crystals have been measured and correlated.

There are few studies on the growth of K_2SO_4 crystals from aqueous solution. Mullin and Gaska (*8*) and Rosen and Hulburt (*13*) reported that the overall K_2SO_4 crystal growth process is of second order with respect to the concentration difference, but Ishii and Fujita (*6*), Randolph and Rajagopal (*12*), and Ishii (*5*) stated that the crystal growth process consists of the two steps in series: diffusion of the solute from the bulk mother liquor to the crystal–liquid interface and interfacial crystallization in which the solute at the interface enters the crystal lattice. They reported that for K_2SO_4 both steps are first order with respect to the concentration difference, and thus the overall K_2SO_4 crystal growth process is first order. The overall crystal growth rate constant obtained by Rosen and Hulburt (*13*) includes the linear velocity of the mother liquor, but the linear velocity of the mother liquor ought not to affect the interfacial crystallization process but only the diffusion process, which is always of first order with respect to the concentration difference. According to Moyers and Randolph (*7*), for any kind of crystals the crystal growth rate can be always approximated by a first order in the case of low supersaturation concentration. Therefore, the difference of the reaction order for the K_2SO_4 crystal growth process among the different authors may be dependent on different supersaturation concentration ranges.

Of course, the reaction order of the crystal growth process must be dependent upon the type of crystal surface and its physical nature such as kinks and imperfect crystal lattices. To encourage more precise experimental measurements for K_2SO_4 crystal growth rate, the properties of aqueous K_2SO_4 solutions and crystals have been here reported.

Knowledge of the properties of the supersaturated solution is essential for studies on K_2SO_4 crystallization and can be obtained by extrapolation from the figures of this paper.

High-purity K_2SO_4 crystals were obtained from the Kokusan Chemical Works Ltd., and ion-exchanged water was used.

Experimental Sections and Correlations

(1) Saturation Concentration. The saturation concentration of aqueous K_2SO_4 solution had been measured in the previous study (*6*), in which the solution and growth rates of K_2SO_4 crystals in stirred tanks were measured.

Figure 1 shows a schematic diagram of the experimental apparatus. The stirred tank and the outer jacket were made of Pyrex glass to make visible the inside of the stirred tank. The dimensions of the stirred tank are shown in Table I. The diameter of the stirred tank, having four baffle plates, is 10 cm. For the depth of the solution to equal approximately the diameter of the stirred tank, 700 cm^3 of the aqueous K_2SO_4 solution was maintained unsaturated, but near the saturation concentration (about 5 °C higher than the saturation temperature), to prevent all crystals from precipitating from solution. The solution temperature was kept at a constant temperature of about 10, 15, 20, 25, 30, 35, 40, 45, or 50 °C for each run by flowing the thermostat water into the outer jacket of the stirred tank and measuring with a calibrated thermometer. Twenty grams of highest quality K_2SO_4 crystals of −3.5+4, −6+7, −8+9, −10+12, −16+20, −28+32, −48+60, −60+65, or

* Author to whom correspondence should be addressed at the Department of Chemical Engineering, Yokohama National University, Ooka, Minami-ku, Yokohama, Japan

0021-9568/78/1723-0019$01.00/0

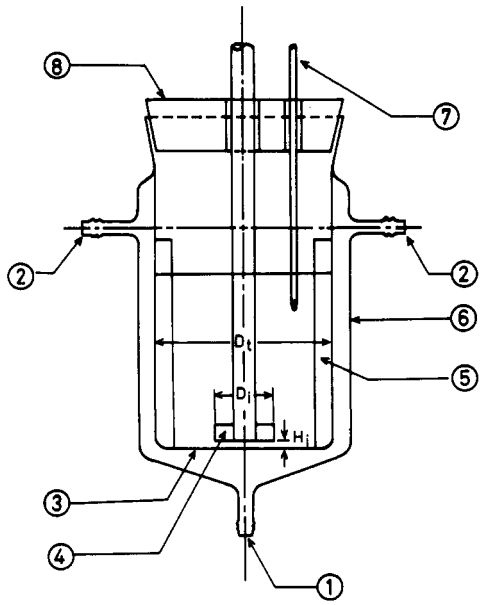

Figure 1. Batch stirred tank.

−100+150 JIS mesh was carefully dissolved in the stirred tank and at given time intervals about 2 cm^3 of the solution was sampled and weighed, and then evaporated, dried, and again weighed. The sampling was made by a fountain pen filler, the mouth of which was tightly sealed with sanitary cotton to prevent crystals from entering. The concentrations of the solutions were determined gravimetrically from the weights of the solutions and the crystals before and after evaporation and drying, respectively. Since the crystal growth rate is slower than the crystal dissolution rate, the saturation concentrations were determined by crystal dissolution experiments; it is difficult to arrive at saturation concentrations in crystal growth experiments. To determine the crystal dissolution rate, it is adequate to carry out the experiments within a 20-min period. However, to determine the saturation concentration the experiments were continued from 2 to 6 h, when the solution concentrations in the stirred tank were essentially at saturation level.

The experimental saturation concentrations and values estimated from the polynomial by the method of least squares are presented in Table II, were plotted as shown in Figure 2, and are correlated by the least-squares method to yield

$$C_s = R_0 + R_1 t^1 + R_2 t^2 + R_3 t^3 + R_4 t^4 + R_5 t^5 + R_6 t^6 + R_7 t^7 \quad (1)$$

Each coefficient of eq 1 is given in Table III. The standard deviation was calculated by the following equation and is very small.

$$\Delta = \left[(1/13) \sum_{i=1}^{13} (C_{si} - C_s)^2 \right]^{1/2} = 0.0185$$

Table II. Saturation Concentration

Temp, °C	Solubility (g of solute/ 100 g of H_2O)	Values estimated by the least-squares method
10.55	9.335	9.334 545
10.56	9.337	9.336 755
14.60	10.16	10.190 28
14.80	10.26	10.230 60
19.80	11.16	11.184 40
19.99	11.25	11.218 87
24.39	11.99	11.998 66
24.49	12.01	12.016 20
30.00	13.03	13.012 49
35.12	13.99	14.005 54
39.76	14.90	14.892 27
45.38	15.81	15.812 41
50.00	16.67	16.669 68

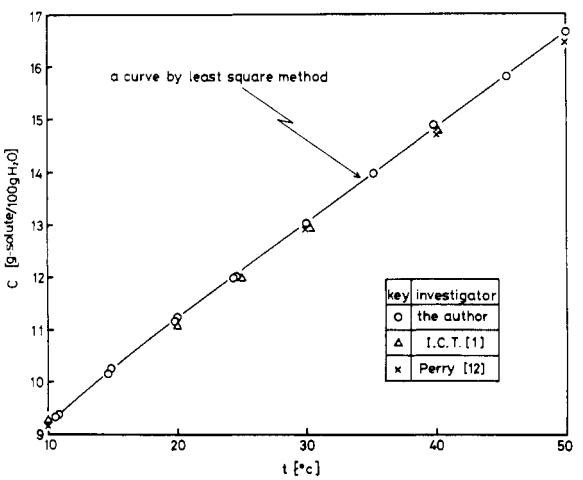

Figure 2. Saturation concentration of K_2SO_4 aqueous solution.

Table III. Coefficient of a Polynomial of Seventh Order by the Least-Squares Method

	Coefficients		Coefficients
R_0	$0.617\,295\,0 \times 10^{1}$	R_4	$-0.160\,719\,2 \times 10^{-3}$
R_1	$0.495\,625\,2 \times 10^{0}$	R_5	$0.454\,189\,9 \times 10^{-5}$
R_2	$-0.391\,644\,5 \times 10^{-1}$	R_6	$-0.659\,812\,6 \times 10^{-7}$
R_3	$0.321\,458\,9 \times 10^{-2}$	R_7	$0.381\,327\,2 \times 10^{-9}$

In Figure 2 the author's data are seen to agree very well with those of I.C.T. (*1*) and Perry (*9*). However, the data of I.C.T. and Perry are slightly lower than the author's data, as seen for example from Figure 3 which is an enlarged portion of Figure 2.

The concentration of the solution in the stirred tank almost reached the I.C.T. and Perry level in 1 h after the start of the experiment, but after 1 h the value continued to increase slightly. Therefore, for the concentration of solution to arrive completely to the saturation level, 2–6 h are required.

Generally, in the experiments on crystal growth the supersaturation concentration of the mother liquor is taken as only

Table I. Dimensions and Conditions of Batch Stirred Tanks

D_t, mm	D_i/D_t	H_i/D_t	Impeller type	Impeller no.	Impeller angle, deg	Impeller material	Baffle width	V_r, L	D_p
100	1/3	1/30	Paddle	2	90	Bakelite	1/10 D_t	0.700	3.5–150 mesh 20 g

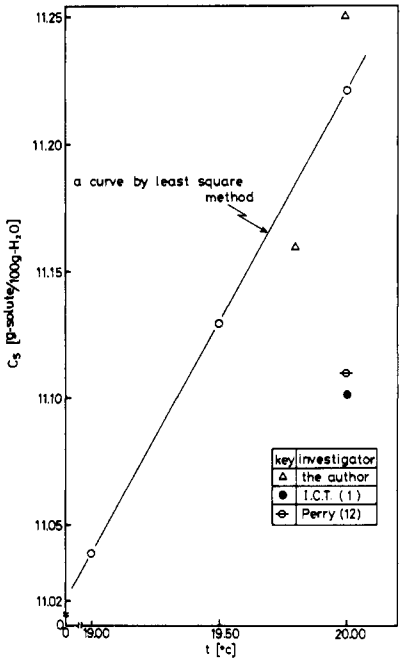

Figure 3. Saturation concentration near 20 °C.

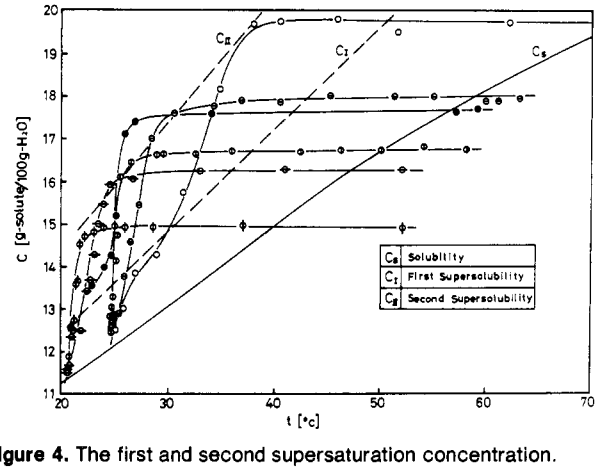

Figure 4. The first and second supersaturation concentration.

Table IV. Densities of Solution

t, °C	c (g of solute/ 100 g of soln)	ρ_L, g/cm^3
30.00	11.07	1.086 64
40.28	12.06	1.090 80
50.00	12.06	1.086 61
50.00	14.09	1.103 78
60.22	13.11	1.089 89
60.22	15.15	1.108 10

slightly larger than the saturation concentration. Therefore the small difference of the saturation concentration has a large effect on the driving force for crystal growth and on the difference between the supersaturation concentration of the mother liquor and the saturation concentration, namely, kinetic data of crystal growth. Therefore, precise data on the saturation concentration are very valuable.

(2) The First and Second Supersaturation Concentration. The first and second supersaturation concentrations of aqueous K_2SO_4 solutions were measured by Tanimoto's method, which as been described in detail (ref 15).

According to this method, 750 cm^3 of introduced K_2SO_4 solution at elevated temperature had been introduced into the same

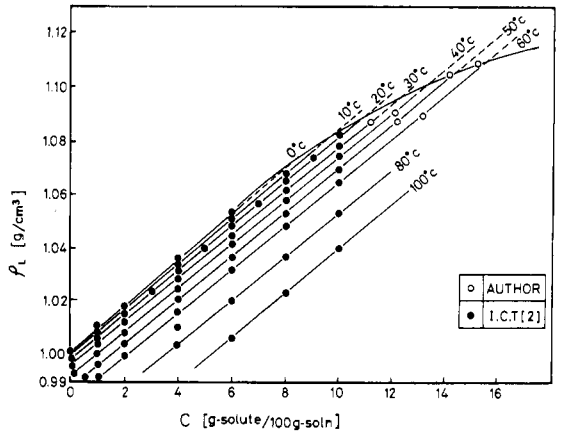

Figure 5. Density of K_2SO_4 aqueous solution.

Table V. Viscosities of Solution

t, °C	c (g of solute/ 100 g of soln)	μ_L, cP
25.14	10.23	1.025
30.00	11.07	0.933
40.28	11.07	0.767
40.28	12.06	0.771
50.00	11.07	0.650
50.00	12.06	0.660
50.00	14.09	0.681
60.22	11.07	0.555
60.22	12.06	0.563
60.22	14.09	0.573

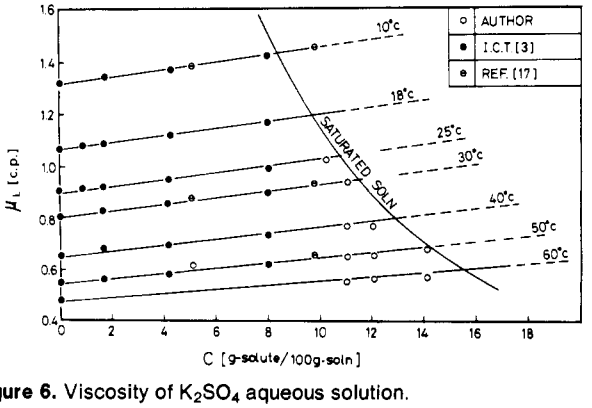

Figure 6. Viscosity of K_2SO_4 aqueous solution.

stirred tank as used to determine the saturation concentration (*5*). The tank had a diameter of 10 cm, was stirred by a 3.33-cm long impeller at a speed of 750 rpm, and cooled by flowing tap water into the outer jacket of the tank at a flow rate of 30 cm/s; the temperature and concentration of the aqueous K_2SO_4 solution in the tank were measured (the latter gravimetrically as described above in part 1, Saturation Concentration) at given time intervals.

Solution concentration varied with time corresponding to the temperature variation with time and the concentrations at which the slope $dc/d\theta$ or $dt/d\theta$ varied slightly and abruptly. These were determined as the first and second supersaturation concentrations.

The supersaturated solution having a concentration between intermediate saturation and the first supersaturation concentration is metastable under the severe conditions of stirring employed.

Figure 4 shows a plot of the experimental data on the first and second supersaturation concentrations.

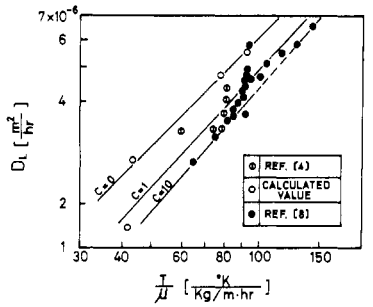

Figure 7. A correlation of diffusitivity of K_2SO_4 in its aqueous solution by Wilke's diffusion factor. c = g of K_2SO_4/100 g of solution.

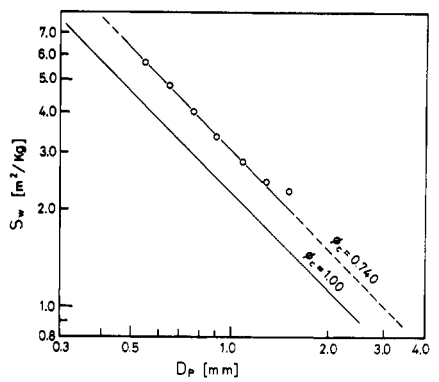

Figure 8. Specific surface area of K_2SO_4 crystals measured by the permeability method.

(3) *Density of Solution.* Densities of concentrated solutions were measured using a pycnometer in a thermostat at constant temperatures of about 30, 40, 50, and 60 °C. They are presented in Table IV and plotted against the solute concentration of the solution in Figure 5. These values agreed fairly with the values extrapolated from the data of I.C.T. (*2*).

(4) *Viscosity of Solution.* Viscosities of concentrated solutions were measured using an Ostwald viscometer in a thermostat at constant temperatures of about 25, 30, 40, 50, and 60 °C. They are presented in Table V and plotted against the solute concentrations of the solution in Figure 6. They agreed well with the values extrapolated from the data of I.C.T. (*3*).

(5) *Diffusivity of Solute.* The data in I.C.T. (*4*) and ref 9 were correlated as shown in Figure 7 according to Wilke's diffusion factor (*13*) with the solute concentration (g of K_2SO_6/100 g of solution) as a parameter. However, the viscosity of the solution was used instead of that of the solvent.

The diffusivities in an infinite dilute solution were estimated from the nature of the electrolytic solution (*10*), plotted in the same figure, and are, of course, larger than those in concentrated solutions at each temperature. The data of the equivalent ion conductance in infinite dilution in ref 16 were used for this estimation.

(6) *Specific Surface Area and Shape Factors of K_2SO_4 Crystals.* Specific surface areas of K_2SO_4 crystals were measured using the permeability method (*11*).

The pressure drops for the laminar flow range through the 2.85-cm i.d. and 10-cm highly packed beds with the sieve fractions of −10+12, −12+14, −14+16, −16+20, −20+24, −24+28, and −28+32 JIS mesh, air-flow rates, and void fractions of the bed were measured. The void fractions were 0.427, 0.416, 0.424, 0.429, 0.426, 0.422, and 0.401, respectively. The air-flow rates ranged from 10.2 to 94.5 cm^3/s.

The specific surface areas were calculated from the following Carman–Kozeny equation based on the assumption that K = 4.5.

Table VI. Shape Factor ϕ'

Size [JIS $_{mesh}$]	ϕ'
−7 + 8	3.75
−9 + 10	3.62
−14 + 16	3.76
−20 + 24	4.21
−24 + 28	4.16
Av	3.90

$$S_w = \frac{g_c}{K\mu_G u_0 \rho_P^2} \frac{\Delta p}{L} \frac{\epsilon^3}{(1-\epsilon)^2} \quad (2)$$

According to the relationship below, the specific surface areas thus obtained were plotted against the particle diameters as shown in Figure 8 and a result of ϕ_c = 0.740 was obtained.

$$S_w = 6(1-\epsilon)/\phi_c D_P \rho_P \quad (3)$$

The weights of 100 crystals of −3.5+4, −7+8, −9+10, −14+16, −20+24 or −24+28 JIS mesh were measured three times for each sieve fraction and the shape factors were calculated from the following equation

$$W/\rho_P = \frac{\pi\phi'}{6}(\phi_c D_p)^3 N \quad (4)$$

The experimental shape factors are presented in Table VI and ϕ' = 3.90 was obtained on an average for these particle size ranges.

Glossary

c	solute concentration of solution, g of K_2SO_4/100 g of H_2O or g of K_2SO_4/100 g of soln
C_I	the first supersaturation concentration, g of K_2SO_4/100 g of H_2O
C_{II}	the second supersaturation concentration, g of K_2SO_4/100 g of H_2O
C_s	saturation concentration, g of K_2SO_4/100 g of H_2O
C_{si}	experimental saturation concentration, g of K_2SO_4/100 g of H_2O
D_L	diffusivity of solute in solution, m^2/h
D_p	particle diameter, m, mm
g_c	gravitational conversion factor, kg m/(h^2 Kg)
K	constant in eq 2
L	packed bed height, m
N	number of crystals
Δp	pressure drop, kg/m^2
Δ	standard deviation, g of K_2SO_4/100 g of H_2O
S_w	specific surface area of crystals, m^2/kg
T	absolute temperature, K
t	temperature, °C
u_0	average linear velocity of air based on empty tube, m/h
W	weight of crystals, kg
ϵ	void fraction of packed bed
μ_G	viscosity of air, kg/(m h)
μ_L	viscosity of solution, kg/(m h)
ρ_L	density of solution, kg/m^3
ρ_P	density of crystals, kg/m^3
ϕ_c	shape factor defined by eq 3
ϕ'	shape factor defined by eq 4

Literature Cited

(1) I.C.T., **4**, 239 (1928).
(2) I.C.T., **3**, 24, 88 (1928).
(3) I.C.T., **5**, 17 (1928).
(4) I.C.T., **5**, 68 (1928).
(5) Ishii, T., *Chem. Eng. Sci.*, **28**, 1121 (1973).
(6) Ishii, T., Fujita, S., *Kagaku Kogaku*, **29**, 316 (1965).
(7) Moyers, C. G., Jr., Randolph, A. D., *AIChE J.*, **19**, 1089 (1973).
(8) Mullin, J. W., Gaska, C., *Can. J. Chem. Eng.*, **47**, 483 (1969).
(9) Mullin, J. W., Nienow, A. W., *J. Chem. Eng. Data*, **9**, 526 (1964).

(10) Olson, R. L., Walton, J. S., *Ind. Eng. Chem.*, **43**, 703 (1951).
(11) Ohyama, Y., "Kagaku Kogaku", Vol. 2, Iwanami Shoten, Tokyo, 1967, p 22.
(12) "Perry's Chemical Engineers' Handbook", 3rd ed, 1950, p 108.
(13) Rosen, H. N., Hulburt, H. M., *Chem. Eng. Prog., Symp. Ser.*, **67** (110), 27 (1971).
(14) Randolph, A. D., Rajagopal, K., *Ind. Eng. Chem., Fundam.*, **9**, 165 (1970).
(15) Tanimoto, A., Kakogi, H., Oota, K., Fujita, S., *Kagaku Kogaku*, **26**, 1239 (1962).
(16) The Electrochemical Society of Japan, "Denkikagaku Benran", Maruzen, Tokyo, 1954, p 122.
(17) The Japan Chemical Society, "Kagaku Benran", Maruzen, Tokyo, 1958, p 481.
(18) Wilke, C. R., *Chem. Eng. Prog.*, **45**, 218 (1949).

Received for review April 19, 1976. Resubmitted January 21, 1977. Accepted June 14, 1977.

Extraction of Acetonitrile from Aqueous Solutions. 1. Ternary Liquid Equilibria

C. Venkata Siva Rama Rao, K. Venkateswara Rao,* A. Raviprasad, and C. Chiranjivi
Department of Chemical Engineering, Andhra University, Waltair, India

Ternary liquid equilibrium data at 31 °C for the system water–acetonitrile–chlorobenzene, water–acetonitrile–xylene, and water–acetonitrile–*n*-butyl acetate are presented. The tie-line data are well correlated by the methods of Othmer–Tobias and Hand. The selectivity increases in the order xylene, chlorobenzene, and *n*-butyl acetate. The system water–acetonitrile–chlorobenzene exhibits solutropy.

The importance of phase equilibrium data for ternary liquid systems in the design of any liquid–liquid extraction process need not be over emphasized. The experimental phase equilibrium data are preferred to that from theoretical predictions as the theoretical data do not always represent actual behavior and the basic thermodynamic data for the predictions are not available for several systems.

The separation of acetonitrile from aqueous solutions is of particular interest in wake of the development of significant demand for acetonitrile as a solvent and starting material for syntheses. Hence, in an attempt to find suitable solvents by liquid–liquid extraction in preference to costlier distillation, the phase equilibrium relationships for the ternary systems acetonitrile–water with chlorobenzene, xylene, and *n*-butyl acetate are studied at 31 °C. Xylene (mixed) is reported (*4*) to have been used as a solvent for extracting acetonitrile from aqueous solutions.

Chemicals

Acetonitrile supplied by Sarabhai M. Chemicals is further purified by fractionation and the fraction boiling at 81.7 °C is collected and used. All the solvents are of reagent grade and are used directly without any further purification. Distilled water free from carbon dioxide is used throughout the work. The physical properties of the chemicals are given in Table I.

Experimental Procedure

The mutual solubility line (binodal curve) is determined at 31 °C by the method as described by Othmer et al. (*3*); i.e., the solubility line is determined by titration of one binary, solute and water or solute and solvent with solvent or water, respectively, until the appearance of turbidity which indicates the presence of a second liquid phase. In the titrations the amount of the third component required could be reproduced to within 0.2% of the total volume (30 mL).

Table I. Physical Properties of the Chemicals

Chemical	Density at 20 °C, g/mL	Refractive index	Bp at 760 mmHg, °C
Acetonitrile	0.781	1.3420 at 25 °C	81.6
Xylene	0.864	1.4930	137–142
Chlorobenzene	1.1065	1.5220 at 25 °C	131.6
n-Butyl acetate	0.881	1.3898 at 30 °C	126.0

Table II. Mutual Solubility and Tie-Line Data for Acetonitrile–Water–Xylene at 31 °C (values expressed in weight percent)

Mutual Solubility Data					
Xylene	Acetonitrile	Water	Xylene	Acetonitrile	Water
0.7	10.5	88.8	19.4	69.1	11.5
0.8	21.6	77.6	33.6	60.4	6.0
1.0	33.8	65.2	36.1	58.5	5.4
2.3	45.7	52.0	46.9	49.5	3.6
4.4	58.1	37.5	60.8	36.0	3.2
5.2	62.1	32.7	73.1	23.9	3.0
9.4	68.5	22.1	85.5	11.8	2.7

Tie-Line Data					
Water layer			Organic layer		
Xylene	Acetonitrile	Water	Xylene	Acetonitrile	Water
0.4	4.0	95.6	95.4	2.1	2.5
0.7	8.8	90.5	93.7	3.6	2.7
1.0	13.8	85.2	92.5	4.8	2.7
1.0	18.0	81.0	87.6	9.4	3.0
1.2	24.0	74.8	84.8	12.2	3.0
1.2	27.4	71.4	77.3	19.6	3.1
1.5	33.8	64.7	68.4	28.4	3.2

For the determination of the tie-line data, the specific gravities corresponding to the points on the binodal curve are determined and a standard plot is prepared by plotting weight percent acetonitrile vs. specific gravity. Different mixtures of the three components within the heterogenous system are shaken thoroughly in separating funnels and then allowed to settle overnight. The two layers are then separated and weighed. The percent of acetonitrile in each layer is determined from the standard plot described above. The complete compositions of the conjugate layers are estimated with the help of the binodal curve. The precision in the composition measurement of the each phase is estimated to be within ±0.005 weight fraction.

0021-9568/78/1723-0023$01.00/0